Preprint
UCRL-133712

Estimating the Maximum Splat Diameter of a Solidifying Droplet

N. G. Hadjiconstantinou

This article was submitted to
1999 International Mechanical Engineering Congress and Exposition, Nashville, TN, November 14-19, 1999

March 31, 1999

U.S. Department of Energy

Lawrence
Livermore
National
Laboratory

Proceedings of IMECE'99
1999 ASME International Mechanical Engineering Congress and Exposition
November 14-19, 1999, Nashville, Tennesee, USA

ESTIMATING THE MAXIMUM SPLAT DIAMETER OF A SOLIDIFYING DROPLET

Nicolas G. Hadjiconstantinou
Lawrence Livermore National Laboratory
L-228
Livermore, California 94551
Email: hadjiconstantinou1@llnl.gov

ABSTRACT

We present a simple analytical model for the estimation of the maximum splat diameter of an impacting droplet on a subcooled target. This work is an extension of the isothermal model of Pasandideh-Fard et al. (1996). The model uses an energy conservation argument, applied between the initial and final drop configurations, to approximately capture the dynamics of spreading. The effects of viscous dissipation, surface tension, and contact angle are taken into account. Tests against limited experimental data at high Reynolds and Weber numbers indicate that an accuracy of the order of 5% is achieved with no adjustable parameters required. Agreement with experimental data in the limit $We \to \infty$ is also very good. We additionally propose a simple model for the estimation of the thickness of the freezing layer developed at the droplet-substrate contact during droplet spreading. This model accounts for the effect of thermal contact resistance and its predictions compare favorably with experimental data.

NOMENCLATURE

c_p Specific heat per unit mass.
D_0 Initial droplet diameter.
D_m Final disk diameter.
h Final disk thickness.
h_c Contact resistance heat transfer coefficient.
h_f Stagnation point flow heat transfer coefficient.
h_{fg} Latent heat per unit mass.
h_s Solidified layer heat transfer coefficient.
h_t Total heat transfer coefficient.
k Liquid metal thermal conductivity.
k_s Solid metal thermal conductivity.
KE_1 Initial drop kinetic energy.
Nu_c Contact resistance Nusselt number.
Nu_f Stagnation point flow Nusselt number.
Nu_s Solidified layer Nusselt number.
Nu_t Total Nusselt number.
r Radial coordinate.
Re Reynolds number.
s Solidified layer thickness.
$\bar{s}$ Time averaged solidified layer thickness.
s^* Non-dimensional solidified layer thickness ($= s/D_0$).
SE_1 Initial drop surface energy.
SE_2 Final disk surface energy.
Ste Stefan number ($c_p(T_m - T_w)/h_{fg}$).
Ste_T Stefan number based on temperature T ($= c_p(T - T_w)/h_{fg}$).
T Solidified layer final (average) temperature.
T_0 Droplet initial temperature.
T_m Droplet melting temperature.
T_w Substrate temperature.
u Radial velocity.
V Excluded volume.
V_0 Initial droplet velocity.
W Work done on deforming droplet.
We Weber number.

Greek symbols
β $= \rho/\rho_s$
γ Surface tension.
δ Boundary layer thickness.
θ_a Advancing contact angle.
μ Viscosity.
ξ Spread ratio ($= D_m/D_0$).

ρ Liquid density.
ρ_s Solid density.
τ Estimated droplet arrest time.
ω Flow parameter.

INTRODUCTION

In recent years various simple analytical models for the estimation of the maximum splat diameter of an impacting droplet on a subcooled target have been proposed. Such models could prove very useful as preliminary design tools in the rapidly developing field of microfabrication. They can additionally facilitate the understanding of the coupled droplet spreading and solidification dynamics, which will lead to improvements in microfabrication quality. In this paper we present a model that accounts for the effects of surface tension, contact angle, and solidification at the droplet-target interface.

Consider a superheated liquid metal droplet of diameter D_0 and at temperature $T_0 > T_m$, impacting a subcooled solid substrate (temperature $T_w < T_m$) with velocity V_0. We are interested in the limit of small superheat, that is $T_0 - T_m \to 0$ where T_m is the melting temperature. When spreading stops, the droplet has reached the maximum splat configuration in the shape of a thin disk of diameter D_m and height h. We assume that the material has partially solidified: a thin layer of thickness s (averaged over the diameter) at the substrate-droplet interface is now solid at (an average) temperature T, where $T_w < T < T_0$, and the remaining droplet material is molten at T_m. The maximum splat ratio ξ is defined as $\xi = D_m/D_0$. One important assumption used in this work is that the droplet arrest is not governed by solidification, that is the effect of heat transfer and solidification is only secondary to the spread process. This assumption is somewhat limiting, but its wide use in the literature (Madejski, 1976; Bennett and Poulikakos, 1994; Pasandideh-Fard et al., 1998) has shown that is very reasonable for a wide range of controlling parameters. A recent critical review by Bennett and Poulikakos (1994) emphasizes the inadequacy of the Stefan problem approach to capture the freezing kinetics and their effect on the droplet spreading and arrest. Further evidence to this effect is given in the work of Pasandideh-Fard et al. (1998): in addition to showing the Stefan problem approach to be very inaccurate, it also suggests that the thermal contact resistance between the target and the droplet plays an important role in the freezing layer growth. The importance of the substrate properties was also reported in the work of Collings et. al (1989).

The model presented in this paper is an extension of the isothermal model for the maximum spread diameter by Pasandideh-Fard et al. (1996). In the isothermal case the target and droplet are at the same temperature ($T_0 = T_w$) and negligible heat exchange takes place between the two. The isothermal model was extended to the non-isothermal case by the above authors in (Pasandideh-Fard et al., 1998). Although agreement with experimental data was demonstrated, the validity of some of the approximations in that model is questionable. The present paper suggests a more appropriate formulation which also improves agreement with experimental data. We additionally propose a model for the estimation of the thickness of the thin frozen layer at the droplet-target interface that is important for the calculation of the maximum splat diameter.

THE MAXIMUM SPLAT DIAMETER

Isothermal model

We briefly describe the isothermal model presented by Pasandideh-Fard et al. (1996) for completeness. The maximum spread diameter, D_m, can be estimated by using an energy conservation argument: the energy at every instant in time, and hence at the maximum splat diameter configuration (configuration 2), has to equal the initial energy of the drop (configuration 1). This initial energy is equal to the sum of the kinetic energy (KE_1) and the surface energy (SE_1) of the impacting droplet. The kinetic energy is given by:

$$KE_1 = \left(\frac{1}{2}\rho V_0^2\right)\left(\frac{1}{6}\pi D_0^3\right), \tag{1}$$

where ρ is the liquid drop density. The initial surface energy is given by:

$$SE_1 = \pi D_0^2 \gamma, \tag{2}$$

where γ is the surface tension coefficient for the drop in the ambient environment.

The energy at the maximum splat configuration consists of the energy dissipated through the action of viscosity during the spreading process and the surface energy of the maximum splat configuration. The first term has been shown (Pasandideh-Fard et al., 1996) to (approximately) equal

$$W = \frac{\pi}{3}\rho V_0^2 D_0 D_m^2 \frac{1}{\sqrt{Re}} \tag{3}$$

where $Re = \rho V_0 D_0/\mu$ is the Reynolds number. This estimate is obtained by assuming an axisymmetric stagnation point flow which in the high Reynolds limit can be

approximated by a viscous boundary layer of thickness $\delta = 2D_0/\sqrt{Re}$, and potential flow outside this boundary layer.

The surface energy (SE_2) is estimated by assuming that the final configuration approximates a thin disk. It is shown by Collings et al. (1989) that given the contact angle (θ_a), and the disk-shape geometry assumption with diameter D_m and height h that is small compared to D_m,

$$SE_2 = \frac{\pi}{4} D_m^2 \gamma (1 - \cos\theta_a). \tag{4}$$

Equating

$$KE_1 + SE_1 = W + SE_2, \tag{5}$$

yields an expression for the spread ratio $\xi = D_m/D_0$ which has been shown to reproduce experimental results satisfactorily (Pasandideh-Fard et al., 1996).

It is important to note that the stagnation flow model used for the calculation of the viscous effects predicts that the droplet spreading stops after time τ, where

$$\tau = \frac{8D_0}{3V_0}. \tag{6}$$

This is important since in the non-isothermal case considered below we assume that spreading is inhibited by viscous and surface tension effects and hence, spreading stops at the same time as the isothermal case.

Non-isothermal spreading

In the non-isothermal case, the effects of solidification have been accounted for in the work of Pasandideh-Fard et al. (1998) by including in the above energy balance a fictitious "lost kinetic energy" term. The kinetic energy of configuration 2, however, is already assumed to be zero in the above energy balance. We believe that, although this term results in a spread factor that is in reasonable agreement with experimental data, it does not adequately represent the physics of solidification. The solidification process manifests itself through the latent heat which should enter the energy balance; if thermal effects cannot be included in the model because of the insufficient understanding of their relative importance, the whole of the solidified material can be excluded. We propose a modification to the above energy balance that correctly captures the effect of phase change and results in a similar expression for the spread factor which is, however, not ad-hoc. In what follows we show that the ad-hoc "lost kinetic energy" term can be motivated as part of the solidified material energy which is not included in our modified energy balance.

The effect of phase change is accounted for by applying the energy balance to the liquid that does not solidify. Following Pasandideh-Fard et al. (1998), we estimate the solidified mass as $\pi\rho_s D_m^2 s$. This material is then excluded from the energy balance $KE_1 + SE_1 = W + SE_2$ under the assumption that negligible thermal energy exchange takes place between the solidified and unsolidified parts of the drop. We believe that this assumption is not unreasonable; the high Reynolds number stagnation flow model inside the drop, which gives reasonable results for the viscous heat generation, involves little mixing and mostly entrainment of the fluid from the potential flow region towards the wall ($RePr \sim 100 \gg 1$). The new terms in the energy balance are now:

$$KE_1 = \left(\frac{1}{2}\rho {V_0}^2\right)\left(\frac{1}{6}\pi {D_0}^3 - \frac{\pi}{4}\frac{\rho_s}{\rho} D_m^2 s\right), \tag{7}$$

and

$$W = \frac{\frac{\pi}{6}\rho {D_0}^3 - \frac{\pi}{4}\rho_s D_m^2 s}{\frac{\pi}{6}\rho D_0^3} \frac{\pi}{3}\rho {V_0}^2 D_0 D_m^2 \frac{1}{\sqrt{Re}}, \tag{8}$$

which lead to a new expression for ξ:

$$\xi^2 = \frac{\omega(Re, We, \theta_a, s^*)}{12\frac{We}{\sqrt{Re}}\beta s^*} - \frac{\sqrt{\omega^2(Re, We, \theta_a, s^*) - 24\frac{We}{\sqrt{Re}}\beta s^*(We + 12)}}{12\frac{We}{\sqrt{Re}}\beta s^*}, \tag{9}$$

where

$$\omega(Re, We, \theta_a, s^*) = \frac{4We}{\sqrt{Re}} + 3(1 - \cos\theta_a) + \frac{3}{2}\beta s^* We, \tag{10}$$

$\beta = \rho_s/\rho$, and $s^* = s/D_0$.

Note that the surface terms SE_1, and SE_2 were not corrected for the reduced mass. In the case of SE_1, the correction is of smaller order because surface effects scale as $V^{2/3}$, where V is the excluded volume ($= \pi D_m^2 s/4$). Neglecting this correction should be reasonable in the high Weber number limit for which this model is intended. In the case of SE_2, the existence of a solid layer between the molten material and the substrate will not affect expression (4) if the interfacial energy between the substrate and

the liquid is not significantly different than the interfacial energy between the liquid and the solid metal.

Taking $\beta \approx 1$, we obtain the following results for the three experimental cases (varying subcooled target temperature T_w) presented by Pasandideh-Fard et al. (1998). For $T_w = 240^oC$, $s^* = 0$, $\xi = 3.24$ and the experimental value is $\xi = 3.3$; for $T_w = 150^oC$, $s^* = 0.014$, $\xi = 3.06$, and the experimental value is $\xi = 3.1$; for $T_w = 25^oC$, $s^* = 0.035$, $\xi = 2.8$, and the experimental value is $\xi = 2.9$. The values of s^* used were obtained from the numerical simulations of Pasandideh-Fard et al. A model for the estimation of s^* is given in the next section.

We see that the our model improves the accuracy of the previous model while being based on a more theoretically sound framework. We can now see the physical significance of the "lost kinetic energy" term in Pasandideh-Fard et al. (1998); it results from the exclusion of the solidified portion of the drop (equation (7)) from the energy balance (equation (5)). One assumption used in the above derivation is that the heat generated from the viscous dissipation is uniformly distributed in the drop volume, and hence it is proportionally distributed to the solidified and unsolidified parts of the droplet (equation (7)). The agreement with the experimental data above suggests that this assumption is reasonable, or that its effect is small.

We can alternatively assume that mixing in the droplet is minimal, and hence the heat generated by viscous dissipation is "retained" within the viscous boundary layer thickness. In this minimal mixing case, the ratio of the thickness between the solidified layer and the viscous dissipation boundary layer (δ) is important. The equivalent of equation (7) is now:

$$W = \left(\frac{\frac{\delta}{D_o}}{\frac{\delta}{D_o} + s^*} \right) \frac{\pi}{3} \rho {V_o}^2 D_o D_{max}^2 \frac{1}{\sqrt{Re}}. \qquad (11)$$

When s^* is large, the material close to the wall, which is within the viscous boundary layer, solidifies and $W \to 0$. Conversely, if $s^* \to 0$, then all of the viscous energy generation is included in the part of the droplet that does not solidify. This modified term results in a new expression for ξ:

$$\xi = \sqrt{\frac{We + 12}{\frac{3}{2} We s^* + 3(1 - cos\theta_a) + 4\frac{We}{\sqrt{Re}} \left(\frac{2}{2 + s^* \sqrt{Re}} \right)}}. \qquad (12)$$

This expression gives the following results for the experimental data presented above: for $T_w = 240^oC$, $s^* = 0$, $\xi = 3.24$ and the experimental value is $\xi = 3.3$; for $T_w = 150^oC$, $s^* = 0.014$, $\xi = 3.17$, and the experimental value is $\xi = 3.1$; for $T_w = 25^oC$, $s^* = 0.035$, $\xi = 2.89$, and the experimental value is $\xi = 2.9$. This alternative expression seems to give results comparable in accuracy to the previous one (equation (9)). It seems that equation (9) tends to underestimate the value of ξ, and equation (12) tends to overestimate the value of ξ. The exact physics must be some compromise between the two assumptions leading to equations (9) and (12). Additional experimental data are needed to determine which assumption is most appropriate. For the purposes of the remaining discussion we will use the assumption resulting in equation (9); the results of both equations are well within a reasonable variation of 10%.

It is noteworthy that ξ in equation (9) is not very sensitive to variations in s^*: a change in s^* of the order of 100% results in a change in ξ that is less than 10%. This is very important because the largest uncertainty, both from the experimental point of view and from the theoretical point of view, lies in the estimation of s^*.

Unfortunately experimental data, against which the above model can be tested, are very limited. Although various researchers have performed experiments, very few experiments are presented in a concise way which allows their use for model calibration and evaluation. In the following subsection we present a comparison between the model prediction and experimental data for the case of negligible surface tension. This limiting case presents a good test for any model, primarily because more experimental data are available (Watanabe et al., 1992), and various alternative model predictions have been investigated in this limit (Bennett and Poulikakos, 1994).

Zero surface tension limit

We investigate here the model predictions in the limit $We \to \infty$, that is when surface tension effects are negligible. For $We \to \infty$ equation (9) reduces to

$$\xi = 0.5 Re^{0.25}. \qquad (13)$$

The exponent of 0.25 is very close to the usually quoted exponent of 0.2 (Bennett and Poulikakos, 1994; Pasandideh-Fard et al., 1998; Watanabe et al., 1992). Direct comparison with the experimental data of (Watanabe et al., 1992) reveals that the above equation results is in much better agreement with experimental data than the SMAC (simplified marker and cell) simulation results of Watanabe et al. predicting

$$\xi = 0.82 Re^{0.2}. \qquad (14)$$

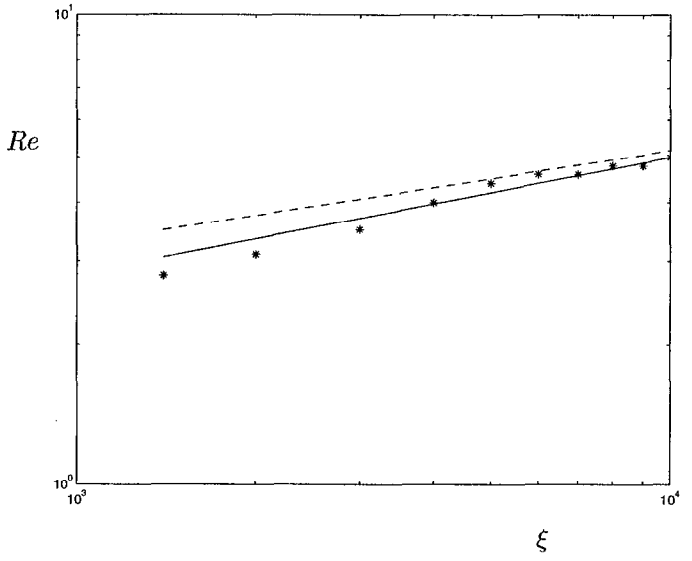

Figure 1. THE SPREAD FACTOR ξ AS A FUNCTION OF THE REYNOLDS NUMBER (Re) IN THE LIMIT $We \to \infty$. THE SOLID LINE REPRESENTS EQUATION (13), THE DASHED LINE REPRESENTS EQUATION (14) AND THE STARS THE EXPERIMENTAL DATA OF WATANABE ET AL.

Further numerical simulations by researchers using the same algorithm (Watanabe et al., 1992) report very similar results ($\xi = 0.83Re^{0.2}$). The Madejski (1976) expression

$$\xi = 1.2941Re^{0.2}, \tag{15}$$

seems to overpredict ξ by a factor of 1.5. The comparison between equations (13), (14), and the experimental data can be seen in Figure 1.

ESTIMATION OF SOLIDIFIED LAYER THICKNESS

The model developed above makes use of the thickness (s) of the solidified layer in contact with the subcooled target. As discussed by Bennett and Poulikakos (1994), and demonstrated through numerical simulations by Pasandideh-Fard et al. (1998), the Stefan problem approach is inadequate. Pasandideh-Fard et al. show that the more involved calculation that includes the effects of contact resistance and substrate temperature can yield fairly accurate results. We present here an alternative and significantly less cumbersome approach to the estimation of this thickness. This approach was chosen because it is the natural extension of the stagnation flow model used for the evaluation of the flow properties of the spreading droplet, and it also lends itself naturally to the estimation of an average (over the splat diameter) thickness. The approach neglects the effects of varying substrate temperature.

We assume that the Stefan number based on the superheat and the melting point is small, that is $c_p(T_0 - T_m)/h_{fg} \ll 1$. This assumption allows us to set the liquid temperature to the melting point temperature T_m and neglect the energy required to cool the superheated drop to this temperature. Equating the energy lost through contact with the substrate to the change in total energy of the solidified part of the drop we obtain:

$$\frac{\pi D_m^2}{4} s\rho_s(h_{fg} + c_p(T - T_w)) = \frac{1}{2}\frac{\pi D_m^2}{4} h_t(T_m - T_w)\tau. \tag{16}$$

The factor of $1/2$ on the right hand side represents the time average of the area available for heat exchange: the velocity with which the droplet spreads is $u \sim \frac{1}{r}$ and hence the area increase rate is linear with time $dA = 2\pi r dr \sim 2\pi u dt$. The final temperature of the solidified layer is an unknown and introduces some uncertainty in our calculation; this issue is further discussed below. The time $\tau = 8D_0/3V_0$ is taken to be the spreading time defined and discussed in the previous section. The total heat transfer coefficient h_t has two contributions:

$$Nu_t = \frac{h_t D_0}{k} = \frac{1}{\frac{1}{Nu_c} + \frac{1}{Nu_f}}. \tag{17}$$

Here $Nu_c = h_c D_0/k$ is the Nusselt number associated with the contact resistance, and $Nu_f = h_f D_0/k$ is the Nusselt number associated with the flow at the stagnation point. The latter can be evaluated (in the $Pr \to 0$, $We \gg 1$ limit) using the correlation for laminar stagnation point flow due to jet impingement on solid targets (Liu et al., 1993)

$$Nu_f = 1.08Re^{0.5}Pr^{0.5}. \tag{18}$$

Note that the thermal resistance associated with the solid layer formed, $1/h_s = \bar{s}/k_s$, is negligible. In the experiments of Pasandideh-Fard et al. (1998), $Nu_s = h_s D_0/k \approx 80$, whereas $Nu_f \approx Nu_c \approx 10$. The above analysis also neglects the effects due to change of the substrate temperature which we feel would be too complex to be incorporated in such a model. Additionally, the encouraging results obtained with the present model suggest that the importance of the substrate temperature variation is small.

Equation (16) leads to

$$s = \frac{4h_t(T_m - T_w)D_0}{3V_0\rho_s h_{fg}(1 + \frac{c_p(T-T_w)}{h_{fg}})}. \tag{19}$$

Temperature T varies between T_m and T_w, and is difficult to evaluate without further assumptions. We define the Stefan number based on this temperature $Ste_T = \frac{c_p(T-T_w)}{h_{fg}}$, such that $0 < Ste_T < Ste$ and equation (19) becomes

$$s^* = \frac{4Nu_t Ste}{3RePr(1+Ste_T)}. \quad (20)$$

When $Ste \ll 1$ it follows that $Ste_T \ll 1$ and the solidified layer temperature has no effect; in the worst case that $Ste \sim 1$, equation (20) provides an upper and lower bound for s^* which differ by at most a factor of 2, which however, as discussed above, result in only 10% uncertainty in ξ.

The above model is used to reproduce the numerical simulation results of Pasandideh-Fard et al. (1998). In these simulations Nu_c=6.8, $Re = 1.2 \times 10^4$, $We = 71$, and $Pr = 0.0073$. For $T_w = 150°C$ ($Ste = 0.324$) the numerical simulations give $s^* = 0.014$ and equation (20) gives $0.015 < s^* < 0.02$, whereas for $T_w = 25°C$ ($Ste = 0.774$) the numerical simulations give $s^* = 0.035$ and equation (20) gives $0.027 < s^* < 0.047$.

CONCLUSIONS

We have developed a model for the approximate calculation of the maximum splat diameter resulting form a superheated liquid metal droplet impacting a subcooled flat surface. The model originates in the work of Pasandideh-Fard et al. (1996, 1998) that successfully addressed the isothermal case; the current work re-addresses the issue of the effect of solidification on the splat diameter that we feel would benefit from an improved representation. The model accounts for the effects of surface tension, viscous dissipation, and contact angle. Good agreement with experimental results available is obtained.

A simple method to estimate the solidified layer thickness that allows for the importance of thermal contact resistance between the substrate and the liquid droplet is also proposed. Comparison with numerical simulations reveals good agreement, making it a preferable method compared to numerical simulations or more involved analytical methods. More thorough tests are required for both models, since the experimental data available to the author are limited.

ACKNOWLEDGMENT

The author would like to thank A. Shapiro for bringing this problem to his attention. This work was perfomed under the auspices of the U.S. Department of Energy under contract W-7405-ENG-48.

REFERENCES

Bennett, T., Poulikakos, D. Splat-quench solidification: estimating the maximum spreading of a droplet impacting a solid surface. Journal of Material Science 1993;28:963-970.

Collings, E.W., Markworth, A.J., McCoy, J.K., Saunders, J.H. Splat-quench solidification of freely falling liquid-metal drops by impact on a planar substrate. Journal of Material Science 1990;25:3677-3682.

Liu, X., Gabour, L.A., Lienhard V, J.H. Stagnation point heat-transfer during impingement of laminar liquid jets: analysis including surface tension. Journal of Heat Transfer 1993;115:99-105..

Madejski, J. Solidification of droplets on a cold surface. International Journal of Heat and Mass Transfer 1976;19:1009-1013.

Pasandideh-Fard, M., Qiao, Y.M., Chandra, S., Mostaghimi, J. Capillary effects during droplet impact on a solid surface. Physics of Fluids 1996;8:650-659.

Pasandideh-Fard, M., Bhola, R., Chandra, S., Mostaghimi, J. Deposition of tin droplets on a steel plate: simulations and experiments. International Journal of Heat and Mass Transfer 1998;41:2929-2945.

Watanabe, T., Kuribayashi, I., Honda, T., Kanzawa, A. Deformation and solidification of a droplet on a cold substrate. Chemical Engineering Science 1992;47:3059-3065.